This document is confidential and is proprietary to the American Chemical Society and its authors. Do not copy or disclose without written permission. If you have received this item in error, notify the sender and delete all copies.

Synthesis and Characterization of Molybdenum(II) Oxalate – Is this the simplest MOF Containing a Metal-Metal Quadruple Bond?

Journal:	*Inorganic Chemistry*
Manuscript ID	Draft
Manuscript Type:	Article
Date Submitted by the Author:	n/a
Complete List of Authors:	Van Der Sluys, William; Pennsylvania State University, Chemistry Conradson, Steven; Josef Stefan Institute, Complex Matter Anderson, Julie; The Pennsylvania State University, Materials Characterization Laboratory, The Materials Research Institute Bazilevskaya, Ekaterina; Penn State, Gray, Jennifer; Pennsylvania State University, Materials Characterization Laboratory Hogg, Kathryn; Pennsylvania State University, Chemistry Pacheco, Carlos; New Jersey Institute of Technology, Department of Chemistry and Environmental Science Paterno, Ann; Pennsylvania State University, Chemistry Tambourine, Gino; Pennsylvania State University, Materials Characterization Laboratory Wetherington, Maxwell; Penn State, Wonderling, Nichole; Pennsylvania State University, Materials Research Institute Zimudzi, Tawanda; Pennsylvania State University, Materials Research Institute

SCHOLARONE™
Manuscripts

Synthesis and Characterization of Molybdenum(II) Oxalate – Is this the Simplest MOF Containing a Metal-Metal Quadruple Bond?

William G. Van Der Sluys,[‡]* Steven Conradson,[§] Julie Anderson,[◊] Ekaterina A. Bazilevskaya,[◊] Jennifer L. Grey,[◊] Kathryn Hogg, [‡] Carlos N. Pacheco,[¥†] Ann Paterno,[‡] Gino L. Tambourine,[◊] Max Wetherington,[◊] Nichole M. Wonderling,[◊] and Tawanda Zimudzi[◊]

[‡] Department of Chemistry, The Pennsylvania State University, Altoona PA, 16601, United States

[¥] Department of Chemistry, The Pennsylvania State University, University Park PA, 16801, United States

[◊] Materials Characterization Laboratory, The Materials Research Institute, The Pennsylvania State University, University Park, 16801, United States

[§] Department of Chemistry, Washington State University, Pulman WA, 99164, United States and the Department of Complex Matter, Jozef Stefan Institute, 1000 Ljubljana, Slovenia

KEYWORDS Quadruple bonds, molybdenum, oxalate, and MOF.

Supporting Information Placeholder

ABSTRACT: Molybdenum(II) oxalate monohydrate has been prepared by two synthetic routes. Refluxing molybdenum(II) acetate with oxalic acid in aqueous solution for extended periods of time, results in the formation of a red-powder (**1**). This material appears to have an empirical formula approximated by $MoC_2O_4.H_2O$, but based on IR spectroscopy and combustion elemental analysis, the solid appears to incorporate carboxylic acid groups. Washing this solid with basic aqueous solutions removes the carboxylic acid groups and produces a maroon powder (**2**). The later material can also be prepared directly from tetrapotassium octachlorodimolybdate, by refluxing with potassium oxalate in aqueous solution, or by hydrothermal methods. Material **2** has been characterized by a variety of methods, including combustion elemental analysis, IR, TGA, MAS-NMR, UV-Vis/near-IR, Raman, SEM, TEM, EXAFS and pXRD. The data suggests that the solid consists of amorphous or possibly nanocrystalline particles in which the quadruply bonded Mo_2^{4+} units are connected by oxalate linkers forming a relatively small two-dimensional oligomer or small coordination polymer (MOF). In addition, the layers are connected by the axially coordinated water molecules, which interact with the oxalate oxygen atoms in the various layers by way of hydrogen bonding. While electronic structure calculations have suggested that this material should have extensive electronic communication between the quadruply bonded Mo_2^{4+} units, by way of conjugation through the oxalate π-orbital system, the relatively small nature of this coordination oligomer potentially limits the utility of this materials for use as a novel electronically conducting material.

Introduction

We have recently become keenly interested in the synthesis of metal organic framework (MOF) type materials that contain metal-metal multiple bonds.[1] The iconic paddle-wheel structures of molybdenum(II) carboxylates (Fig 1)[2,3] represents an intriguing synthon for the preparation of carboxylate based MOFs.[4] Besides the well-studied properties typically observed for MOF type materials, such as gas and small molecule adsorption[5,6,7] as well as catalysis,[8] we are particularly interested in the potentially novel electronic properties that these materials might possess.[9]

Chisholm and Cotton have shown that it is possible to link quadruply bonded dinuclear units using simple carboxy anions, such as oxalate and squarate to form dimers of dimers that exhibit varying degrees of electronic communication between the dinuclear metal units by way of the π-system of the linking carboxy anions.[10] These relatively simple linkers can be used to produce a variety of oligomers, such as triangular trimers of

dimers and square tetramers of dimers.[11] Perhaps of even greater interest, are the possibility of forming one- and two-dimensional coordination oligomers and polymers, as shown in Fig. 2.

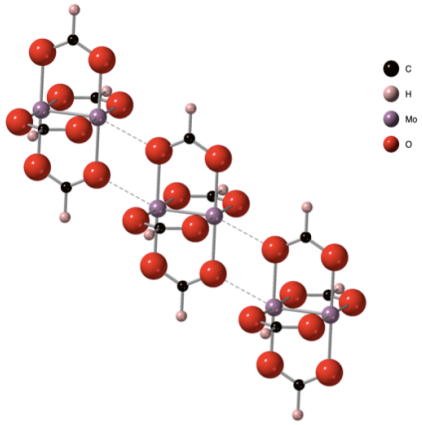

Figure 1. The paddle-wheel structure of dimolybdenum(II) tetraformate,[2] emphasizing the weak interactions of formate oxygen atoms with the axial positions of the Mo_2^{4+} ions.

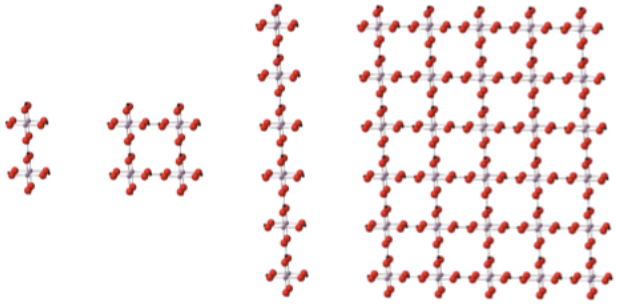

Figure 2. Depictions of some oxalate linked quadruply bonded Mo_2^{4+} oligomeric structures: (a) a dimer of dimers; (b) a square tetramer of dimers; (c) a one-dimensional hexamer; and (d) a two-dimensional oligomeric structure.

Chisholm and coworkers have speculated about the existence of higher order oligomers, noting that trans-substitution of carboxylate ligands would result in one-dimensional polymers and cis-substitution would result in small molecular square tetramers of dimers.[12] Theoretical studies have suggested a significant degree of electronic delocalization in these oligomeric species.[13] It may be anticipated that there will be weak axial interactions, similar to that observed in molybdenum(II) formate (Fig. 1).[2] In a two-dimensional MOF, the interactions between layers, in which an oxalate oxygen atom loosely interacts with neighboring molybdenum atoms, may well produce sheet-like structures analogous to graphene and graphite.[14] In addition to the potential for the cavities to act as hosts for the incorporation of small molecules, it may be possible for Lewis bases such as water, to coordinate to the metals in the axial positions, as seen in chromium(II) acetate hydrate, which could facilitate hydrogen bonding interactions between the sheets.[15]

There has been considerable interest in the nature of the organic linker in MOF type materials and the linker's influence on the electronic communication between the metal centers.[4] Chisholm and Lear have studied the electronic communication in the oxalate bridged dimer of dimers, supported by ancillary pivalate ligands, in both its neutral and singly oxidized states, and suggest that the data is consistent with a class III (totally delocalized) Robin and Day categorization.[16] Unfortunately, there is a dearth of information in the literature concerning the synthesis and properties of molybdenum(II) oxalate, which might represent this highly desirable MOF.[5,17,18]

Recently, we reported our attempt to prepare molybdenum(II) squarate, by the reaction of molybdenum(II) acetate or octachlorodimolybdate with squaric acid and sodium squarate, under anaerobic hydrothermal reaction conditions, which did not produce a coordination polymer, but instead resulted in oxidation of the molybdenum atoms to produce a molecular dinuclear molybdenum(III) hydroxysquarate species. This product is structurally similar to the previously known chromium(III) species, except that the molybdenum(III) hydroxysquarate has a somewhat unusual metal-metal single bond with a $\sigma^2\pi^2\delta^{*2}$ electronic configuration.[19] In this paper we wish to report our efforts to prepare molybdenum(II) oxalate.

Results and Discussion

Synthesis and Characterization

Molybdenum(II) acetate was ground to a fine powder, prior to reaction with excess of oxalic acid in refluxing deoxygenated aqueous solution for several days. As shown in Scheme 1, this produced an extremely insoluble bright red powder (**1**), which based on infrared spectroscopy (Fig. 1) appeared to no longer contain acetate.

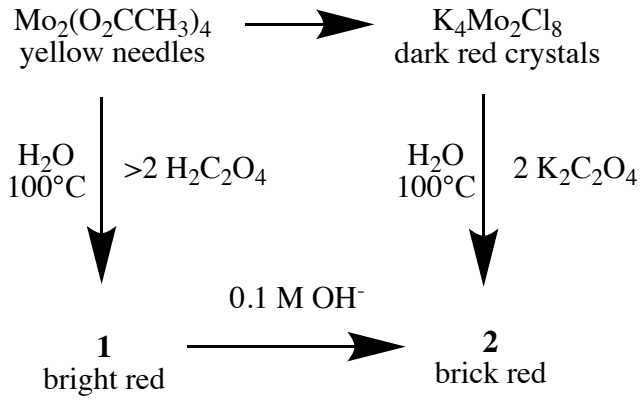

Scheme 1. Synthetic approaches for the preparation of $MoC_2O_4{\cdot}H_2O$ (**1** and **2**).

Table 1. Duplicate combustion elemental analysis data for **1** and **2** as compared with the theoretical percentages for the empirical formula $MoC_2O_4{\cdot}H_2O$.

Cmpd.	C %	H %	N %
1	12.50, 12.52	1.59, 1.62	-
2	11.12, 11.28	0.93, 1.02	-
$MoC_2O_4{\cdot}H_2O$	11.893	0.998	-
3	24.3, 24.33	3.32, 3.43	5.72, 5.71
MoC_2O_4.DMF	23.36	2.74	5.45

Combustion elemental analysis of **1** suggested an empirical formula of $MoC_2O_4{\cdot}H_2O$, but the carbon and hydrogen percentages are slightly higher than the theoretical values, as shown in Table 1.

The relatively simple infrared spectrum of **1** (Fig.3) compares well with calcium oxalate monohydrate (COM).[20] The prominent vibrations associated with the oxalate anion and the broad hydrogen bonded O-H stretching (3435 cm^{-1}) and bending modes (1636 cm^{-1}) of the water are clearly observed. The latter is sensitive to the degree of hydrogen bonding and the nature of the cation. The bending modes are often obscured by the C=O stretching vibrations. The most notable difference between **1** and COM is the somewhat weak vibration at 1735 cm^{-1}, which we suggest is due to the presence of uncoordinated carboxylic acid groups, perhaps due to the presence of hydrogen oxalate at the surface of the crystallites, or possibly the incorporation of a small amount of excess oxalic acid into the cavities of the material. However, if the later were true, we would expect to observe a sharp non-hydrogen bonded O-H stretch around 3600 cm^{-1}, similar to when excess terephthalic acid is trapped in the pores of MOFs like MIL-53as.[21]

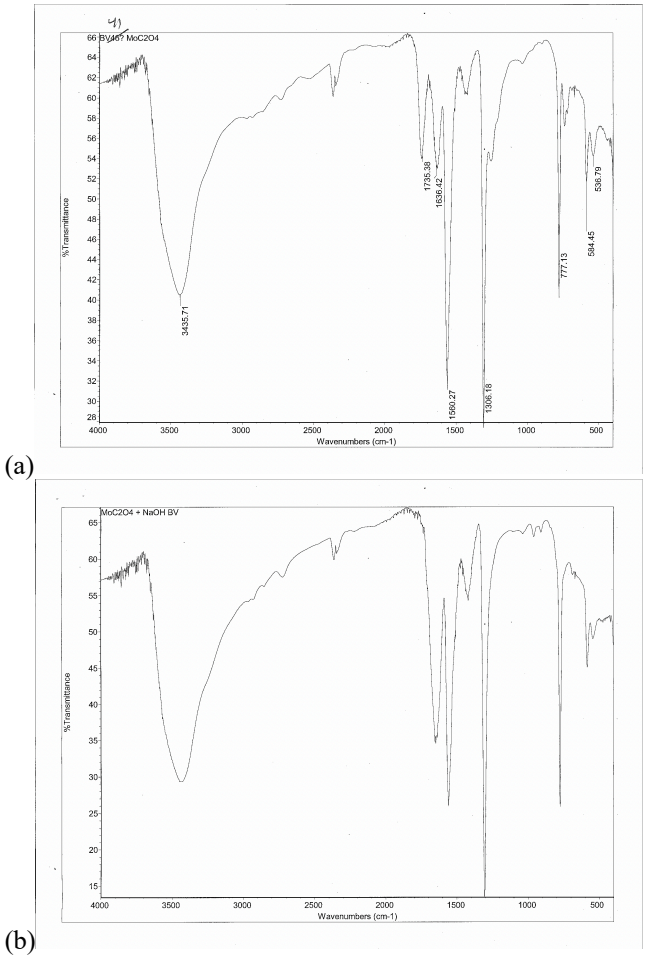

Figure 3. IR spectra of (a) **1** and (b) **2** produced by washing **1** with a 0.10 M KOH solution. The vibration at 2349 cm^{-1} is the asymmetric carbon dioxide stretching mode due to incomplete background subtraction of air.[22]

Sykes and coworkers have studied the substitution reaction kinetics between oxalate and the dimolybdenum(II) aquo ion.[23] The highly oxygen sensitive Mo_2^{4+} (aq) ion can be prepared from molybdenum(II) acetate, by going through a series of intermediates, including the octachlorodimolybdeate (OCDM, $Mo_2Cl_8^{4-}$),[24] and the dimolybdenum(II) tetrasulfato ion.[25] When the Mo_2^{4+} (aq) ion was reacted with excess oxalate at pH = 1, first order reaction kinetics were observed and an orange-red solid was produced, reportedly having an infrared band at 1740 cm^{-1}. This vibration was attributed to the presence of hydrogen oxalate ligands. No further structural information concerning this solid was provided. It is more than likely that this solid is essentially the same material that we have produced by reacting oxalic acid with molybdenum(II) acetate (Scheme 1).

Washing **1** with dilute degassed potassium hydroxide solution results in a slight color change, from bright red to maroon (Scheme 1), and produces what appears to be a slightly different material (**2**). We were initially concerned that this color change was due to oxidation of the molybdenum ions, but the IR spectrum of **2** (Fig. 3), does not support this conclusion. The infrared spectrum of **2** is quite similar to **1**, except that it no longer contains the C=O stretch at 1735 cm^{-1}. The combustion elemental analysis of **2** (Table 1) shows a lower carbon and hydrogen percentage than **1**, consistent with the deprotonation of the carboxylic acid groups. In fact, **2** appears to be quite stable to oxidation and can be stored in air for weeks with minimal changes in the infrared spectrum. However, there does appear to be a slow decomposition over the period of months, with the appearance of Mo=O vibrations near 1000 cm^{-1}.

Molybdenum(II) acetate is readily converted into potassium OCDM by reaction with potassium chloride in fuming hydrochloric acid.[26] The later compound is slightly more soluble in aqueous solution and we have been able to easily prepare **2** from OCDM by refluxing with potassium oxalate, in degassed aqueous solution for several hours. Based on SEM and TEM (Fig. 4), the resulting product is nanocrystalline at best, with a lack of clear electron diffraction, suggesting an amorphous material. EDXS of the sample clearly indicates the presence of molybdenum, carbon and oxygen, with minor amounts of potassium and an even smaller amount of chlorine, but reliable quantification of these amounts has been difficult due to the presence of hydrogen in the sample, which does not produce an X-ray spectrum.

We have also prepared **2** from OCDM by way of a hydrothermal approach, using an autoclave at 150°C, but have been unable to prepare a crystalline sample suitable for single crystal X-ray analysis. When water is replaced by other solvents such as DMF, the solid product (**3**) appears to incorporate the solvent, but the crystallinity was not significantly improved based on TEM. We have also tried this hydrothermal approach using aqueous dimethyl oxalate, in hopes that the slow hydrolysis of the ester would facilitate the formation of nucleation sites. Unfortunately, this approach also did not produce improvements in crystalline morphology.

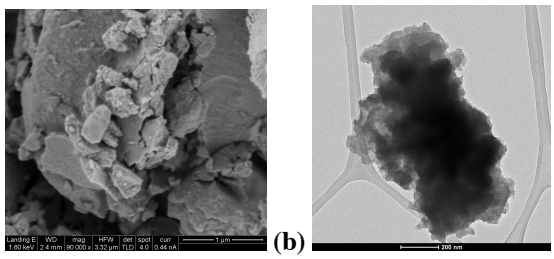

Figure 4. *(a) SEM and (b) TEM images of* ***2****.*

Thermal Analysis

The TGA-MS of **2** (Fig. 5 and supplementary materials) is consistent with the formulation of $MoC_2O_4 \cdot H_2O$. The onset of mass loss occurs at 80°C and slowly continues until there is a dramatic weight loss starting at about 390°C, with no further weight loss, up to 800°C. Exposure of the resulting solid to air results in a weight gain, presumably due to oxidation and the formation of higher molybdenum oxides.[27] The initial percentage weight loss was about 8% and, the total experimental percentage weight loss was approximately 36%. The initial weight loss is due to water, followed by the loss of two equivalents of carbon monoxide (Eqs. 1 and 2), ultimately resulting in the formation of molybdenum(IV) oxide, which theoretically comprises the remaining 63.3% of the original formula. The loss of two equivalents of carbon monoxide contrasts with the TGA of COM, in which there is an initial loss of water, followed by one equivalent of carbon monoxide, and finally a loss of one equivalent of carbon dioxide, to produce calcium oxide.[28] This difference is presumably due to the availability of higher oxidation states for molybdenum.[29]

Similarly, the molybdenum(II) oxalate DMF adduct, slowly loses mass in the range of 50-350 °C, which based on MS is due to DMF and its decomposition products. There is again a dramatic weight loss around 400°C, corresponding to oxalate decomposition, carbon monoxide loss and the formation of molybdenum (IV) oxide. The total experimental weight loss was 54.0 %, which compares fairly well with the theoretical value of 50.2 %.

$$MoC_2O_4{\cdot}H_2O\ (s) \rightarrow MoC_2O_4\ (s) + H_2O\ (g) \quad (1)$$

$$MoC_2O_4\ (s) \rightarrow MoO_2\ (s) + 2\ CO\ (g) \quad (2)$$

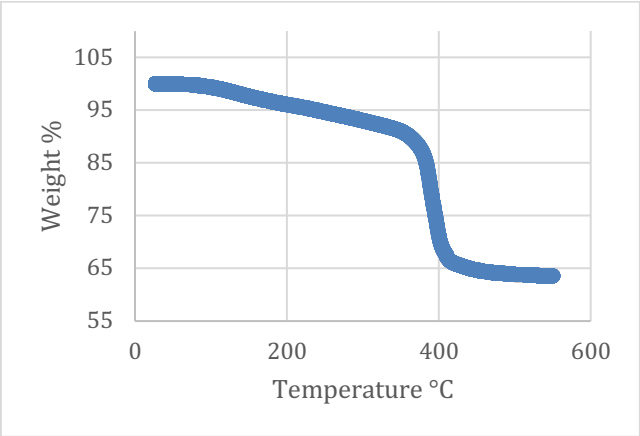

Figure 5. TGA of **2** (blue) and its derivative (green) conducted in an atmosphere of argon.

Electronic Absorption Spectra

The lowest energy electronic absorption in molybdenum(II) carboxylates is the weak δ→δ* transition, which sometimes displays vibrionic fine structure due to coupling with the Mo-Mo stretch. These electronic transitions have historically been the subject of intense debate concerning the electronic structure of metal-metal quadruple bonds.[11,30] The yellow color of these compounds is primarily a result of an intense charge transfer transition, which occurs at higher energy than the δ→δ* transition. This charge transfer transition involves promoting an electron from the δ-orbital, which is the HOMO, to a π*-orbital of the carboxylate ligand.

Chisholm and coworkers[11,12,21] have investigated the electronic structure of the oxalate dimer of dimers and several model oligomeric species using DFT and suggested that the most significant electronic absorptions in the visible portion of the spectrum would be charge-transfer transitions, in which an electron is transferred from a metal-metal δ-type orbital, to the π*-type orbitals of the oxalate ligands. The oxalate ligands produce greater delocalization than in the simple carboxylates, hence the charge transfer transition shifts to lower energy for the oxalate as compared with the corresponding charge transfer for the alkyl carboxylates. This ends up obscuring the δ→δ* transition.[11] As the size of the oligomer increases, it would be reasonable to assume that further conjugation through the metal-based electrons and the extended oxalate π-system, should shift these charge-transfer transitions to even lower energy, perhaps even into the near-IR region. On the other hand, it has been speculated that in a one-dimensional polymer, rotation about the oxalate C-C bond could disrupt this conjugation and thereby prevent extensive electronic delocalization. It has been speculated that in solution, this rotation is the source of the complicated nature of the vibrionic coupling observed in the variable temperature solution spectra of the dimer of dimers.[31] At room temperature this coupling is most prominently observed in the tungsten analogue. In the solid-state linear oligomers, this rotation could effectively produce electronically isolated subunits within the oligomers. It is difficult to imagine how this might occur in a two-dimensional oligomer (Fig. 2d), but presumably this could also occur, hindering the formation of well-defined crystalline solid-state structures.

Shown in Figure 6 is the UV-Vis electronic absorption spectrum of **2** obtained as a KBr pellet. An intense absorption occurs in the visible portion of the spectrum, centered at a wavelength of 480 nm, which interestingly enough, is similar to what was observed for the molybdenum dimer of dimers. We note that DFT theoretical calculations on the linear molybdenum oligomers indicate that the charge transfer band is much less sensitive to the size of the oligomer, than the corresponding tungsten species.[32] While we were unable to determine a molar absorptivity coefficient due to the extreme insolubility of **2**, we did have to make relatively dilute KBr pellets to keep the absorption from going off scale. The intensity of this absorption is consistent with a charge transfer band and the deep maroon color of this material.

We have also looked for significant absorptions in the near-IR region (800-2000 nm) for samples of **2** as KBr pellets, but have been unable to identify any significant absorptions assignable to a charge transfer band.

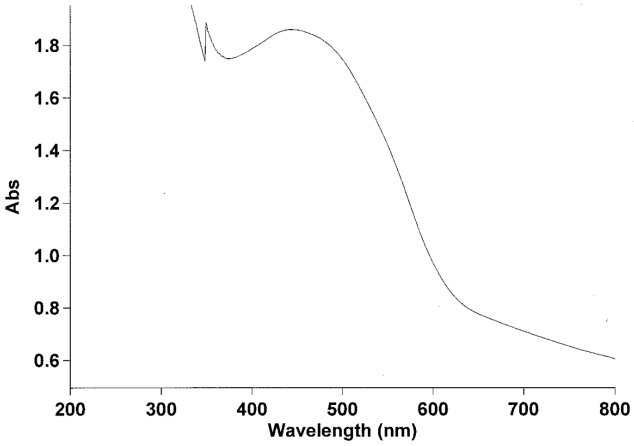

Figure 6. UV-vis spectrum of **2** as a KBr pellet. The discontinuity at 340 nm is due to a grating change.

Raman Spectrum

The Raman spectrum of **2** with excitation at 488 nm is shown in Figure 7, and compares remarkably well with the molybdenum pivalate dimer of dimers, which has been definitively analyzed by Chisholm and coworkers.[21] The most prominent feature of the Raman spectrum of the dimer of dimers is the symmetric C-O stretch (S_1), with weaker C-C stretching (S_2), C-O bending (S_3), combination modes and most importantly, the Mo-Mo stretch at 396 cm^{-1}. The later was consistent with very weak solid-state axial interactions of pivalate oxygen atoms with the molybdenum atoms in neighboring molecules. The most significant aspect of our result is the presence of the Mo-Mo symmetric vibration observed at 383 cm^{-1}.

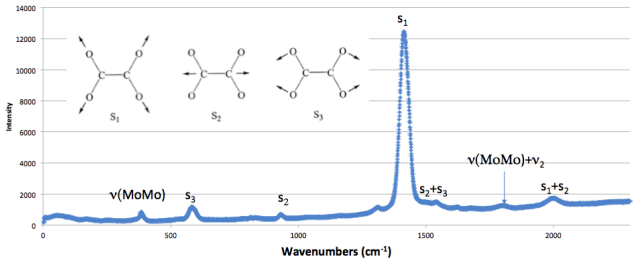

Figure 7. Raman spectrum excited at 488 nm and assigned vibrational modes of **2**.

Raman spectroscopy is a particularly useful tool for probing the nature of Mo-Mo quadruple bonds and the existence of axial Mo-L interactions. Typically, the un-solvated molybdenum(II) carboxylates have Mo-Mo vibrations around 400 cm^{-1}, while the frequencies of the Lewis base adducts shift by as much as 30 cm^{-1} to lower energy, as seen in the pyridine adducts.[33] We feel that the shift of 13 cm^{-1} to lower frequency for **2** as compared with Chisholm's un-solvated molybdenum(II) pivalate oxalate dimer of dimers, suggests a slightly stronger axial interaction, perhaps with the solvated water molecules.

Solid-state MAS NMR

We have obtained the natural abundance carbon-13 solid-state NMR spectrum of **2** (Fig. 8). The chemical shift for the oxalate carbon atoms was centered around 162 ppm, which is in the region typically expected for oxalate carbon signals. This feature is a relatively broad series of resonances with somewhat complex features, consistent with a number of chemically independent carbon atoms that would be expected in an oligomer, or mixture of oligomers. Chisholm and coworkers observed the oxalate carbon-13 signal of the pivalate dimer of dimers at 156.9 ppm.[21]

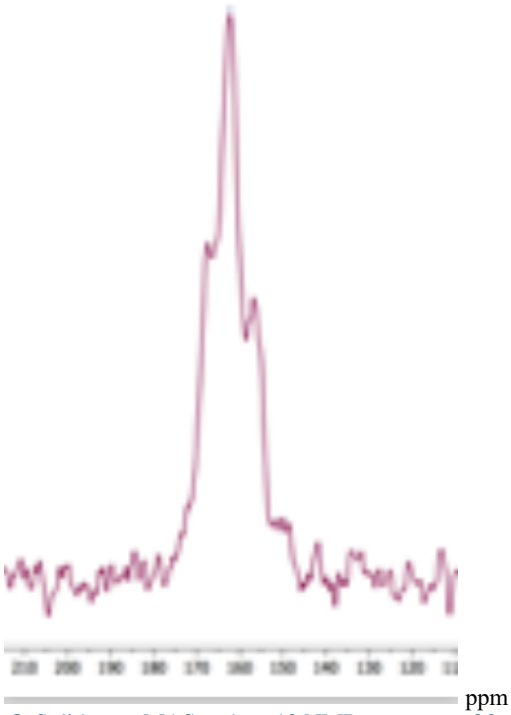

Figure 8. Solid-state MAS carbon-13 NMR spectrum of **2**.

XAFS Analysis

The local environment of the Mo, and in particular the presence and structural parameters of a neighboring Mo, was elucidated by EXAFS at the Mo K edge. EXAFS is arguably the most

direct and incisive method for determining the chemical speciation of a target element in any state of matter and with any degree of disorder in terms of identifying its valence and local symmetry, the elements constituting the neighbor shells to Z±3, and their distances from the central atom to ±0.01-0.03 Å. Its utility in characterizing the speciation of Mo in the solid state and solution has been demonstrated in a number of applications, especially as a component of multi-method analysis incorporating several spectroscopic techniques, as performed here.[34,35,36]

Features on the X-ray Near Edge Absorption Spectrum serve as a fingerprint for geometries and bonding. For molybdenum, the signature of terminal, multiply bound oxygen neighbors that occur with the higher valences is a distinct shoulder on the low energy side of the principal absorption edge. The absence of this feature in the XANES of **2** (see supporting information) indicates the corresponding absence of these types of oxygen, from which a valence state ≤IV can be inferred.[31]

Metrical information was obtained by nonlinear least squares curve-fits of the EXAFS region of the spectrum. Presentation of the EXAFS as the Fourier transform, $\chi(R)$, is most useful because the modulus presents an approximation of the partial radial distribution function. The caveats are: (1) The Z dependent phase shift causes the peaks to be below the actual absorber-neighbor distances; (2) The peak widths are determined by the finite data range of the transform and are therefore much greater than the actual widths of the pair distribution; (3) Destructive interference between the EXAFS waves of similar frequencies in $\chi(k)$ because they originate in neighbor atoms at similar distances can cause their overlapping contributions to $\chi(R)$ to exhibit distortions and substantially reduced amplitudes. However, these unique factors of the EXAFS waves result in the capability of curve-fitting analysis to separate them and provide accurate structural information far exceeding the overall appearance of $\chi(R)$. This last point is accentuated by the total information content of $\chi(R)$ being accessed not by the modulus alone but in combination with either the real or imaginary component. This occurs automatically in the curve-fit in $\chi(k)$ because the EXAFS waves consist of unique amplitudes and phases. Thus, the two peaks at R = 1.4 and 1.9 Å and shoulder at 2.6 Å in the $\chi(R)$ spectrum of **2** (Fig. 9) are fit with one Mo and three neighbors (Table 2 and Fig. 11). The separations between the carbon and oxygen are much greater than the spatial resolution of $\pi/2k_{max}$ = 0.13 Å [k = 13] of the curve-fit, minimizing the correlation between them. The molybdenum is found at virtually the same distance as the nearest oxygen. However, since molybdenum and oxygen have extremely different amplitudes and phases their individual waves are easily deconvoluted by the fit. Proof of the molybdenum neighbor is provided by the excellent correspondence between the wave calculated by the fit using the theoretical Mo-Mo phase and amplitude, and the component of the spectrum that it is fitting (Fig. 11) after isolation by subtracting the waves of the other neighbor shells. Despite this difference in form, the waves are still subject to some degree of interference, shown by the total amplitude of the $\chi(R)$ modulus being reduced from the sum of the two contributions (Fig. 9). For this reason, and in the absence of more precise information on their Debye-Waller factors, we do not report numbers of atoms beyond the observation that they are comparable in overall size and therefore both are required for a good fit.

The types of oxygen and carbon neighbors can be assigned from their distances in comparison with other known molybdenum(II) carboxylate structures.[11,37] The 2.08 Å distance could be to the directly bonded oxygen of the oxalate. The 2.65 Å distances could be to the carbon of the oxalate, which is consistent with bridging oxalates across the Mo-Mo bond forming the prototypical five membered-ring found in a paddle-wheel like structure, rather than bidentate oxalates, bonded

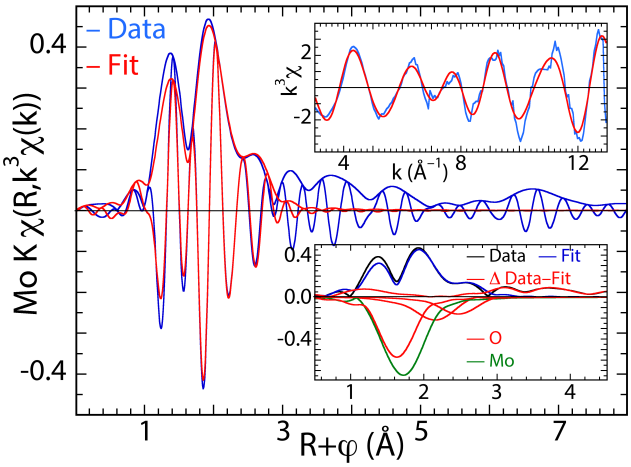

Figure 9. Fourier transformations and fits of the EXAFS data for **2**, plotted as a function of R and k (top inset), with FT moduli and inverted shell contributions, along with a difference between the data and fits (bottom inset).

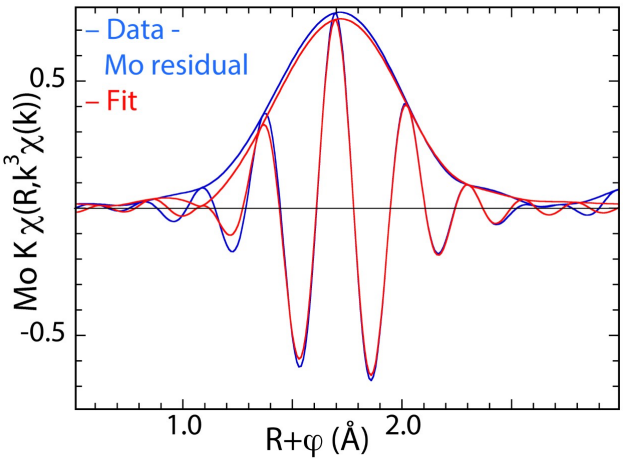

Figure 10. Fourier transformation of the XAFS data and fit for the molybdenum neighbor shell, after subtracting all all other shell contributions.

Table 2. Calculated distances between the target molybdenum atom and near neighbor shells based on the EXAFS data.

Shell	Neighbor atom	Distance (Å)
1	C	2.65
2	Mo	2.10
3	O	2.08
4	O	2.96

to a single molybdenum atom. Alternatively, this distance could also be an axial intermolecular interaction between the molybdenum and oxalate oxygen atoms in neighboring layers, similar to that observed in molybdenum(II) acetate.[38] The oxygen at 2.96 Å is consistent with the distance expected between the molybdenum and an oxalate oxygen atom that is bonded to the molybdenum on the other side of the structure.

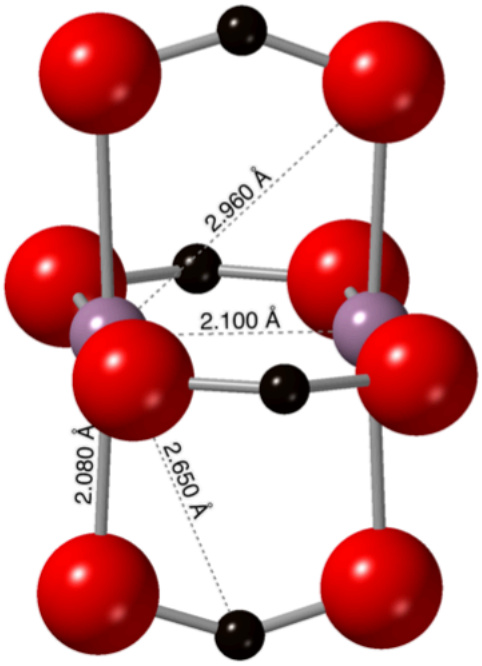

Figure 11. A ball and stick drawing of the MoC_2O_4 structure that would be consistent with the EXAFS data.

The combined thermal and static disorder and possible multiple scattering contributions make fits and assignments of other features resulting from light atoms, overly speculative. However, the most important result is the 2.100 Å Mo-Mo distance which is definitive for the presence of a quadruple bond.

Powder X-ray Diffraction

All attempts to obtain crystals of **2** suitable for single crystal X-ray diffraction were unsuccessful. However, we were able to obtain a pXRD pattern of **2** (Fig. 12), which provided broad diffraction peaks, consistent with a nanocrystalline or nearly amorphous material.[39] This broadening prevented us from using standard techniques for cell indexing and structure determination.

We used the data obtained from the EXAFS experiment as a starting point for the modeling of the pXRD pattern and assumed that there would be a weak interaction of oxalate oxygen atoms with the axial positions of the molybdenum atoms.[31] The best fit for this structure was obtained

using a monoclinic space group (P2), which after Rietveld refinement gave a unit cell of a = 5.98 (2) Å, b = , 6.87 (3) Å, c = 6.96 (3) Å, β = 119.0 (2)°, where R = 6.0 %. We have also obtained nearly identical results using the space group P2/m. The refined distances compare well with the EXAFS distances, with the Mo-Mo, and average oxalate Mo-O distances being 2.09 (2) Å and 2.13 (2)Å, respectively. The axial Mo-O was 2.76 (2) Å, which is in the range (2.6–2.9 Å) typically observed in other molybdenum(II) carboxylates.[11] A slightly better fit was obtained when we used a larger triclinic cell (P_1), where a = 8.2 (1) Å, b = 7.0 (1) Å, c = 7.0 (1) Å, α = 89.6 (9)°, β = 119.6 (5)°, and γ = 89.5 (8)° (R = 5.7%), that included waters of hydration in the axial positions of the Mo-Mo bond. The final refined bond distances again compared well with the EXAFS distances, with the Mo-Mo and average oxalate Mo-O distances being 2.11(1) Å and 2.08(2) Å, respectively, while the axial Mo-O distance for the water was 2.21(1) Å. In this structure, presumably the layers would off-set so that the axial water molecules could connect the layers by way of hydrogen bonding. We have also tried fitting a number of other possible space groups and have also tried to incorporate water molecules in axial positions such that they would connect the layers by way of hydrogen bonding. These structures did not result in an improved fit and generally gave R values of 6-9 %. The diffraction pattern is dominated by the layers of oxalate oxygen and molybdenum atoms, with the coordinated waters and their orientations having minimal effect on the fit. If the waters of hydration are not located in the axial positions, then we assume that they would be located in the cavities of the structure, but we have been unable to develop a model that provides a reasonable fit for this structural type. Figure 13 shows representations of both possible structures. The broad features of the pXRD are difficult to simulate and highly dependent upon the size of the crystal domains we use to model the pXRD. It is likely that there are a range of particle sizes (1-3 nm) and we estimate that the average domain sizes are approximately 2 nm in diameter (see supplementary materials). This would be consistent with a nearly amorphous material with crystalline domains representing oligomers of a few paddle-wheel units in any one direction.

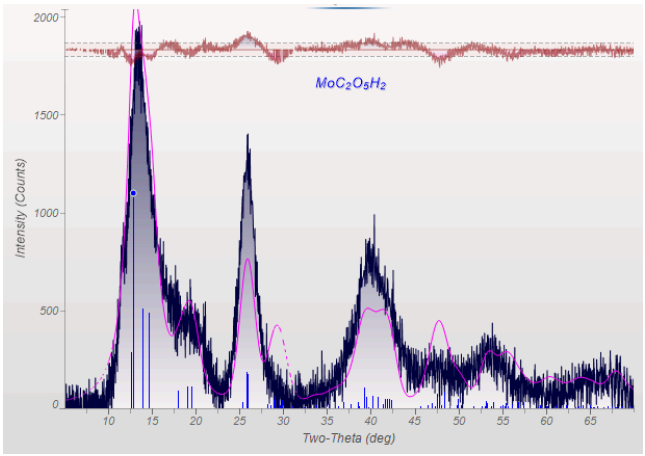

Figure 12. A comparison of the experimental pXRD (black), Rietveld refined simulation (pink) and theoretical hkl line reflections (blue) of **2** with waters of hydration in axial positions.

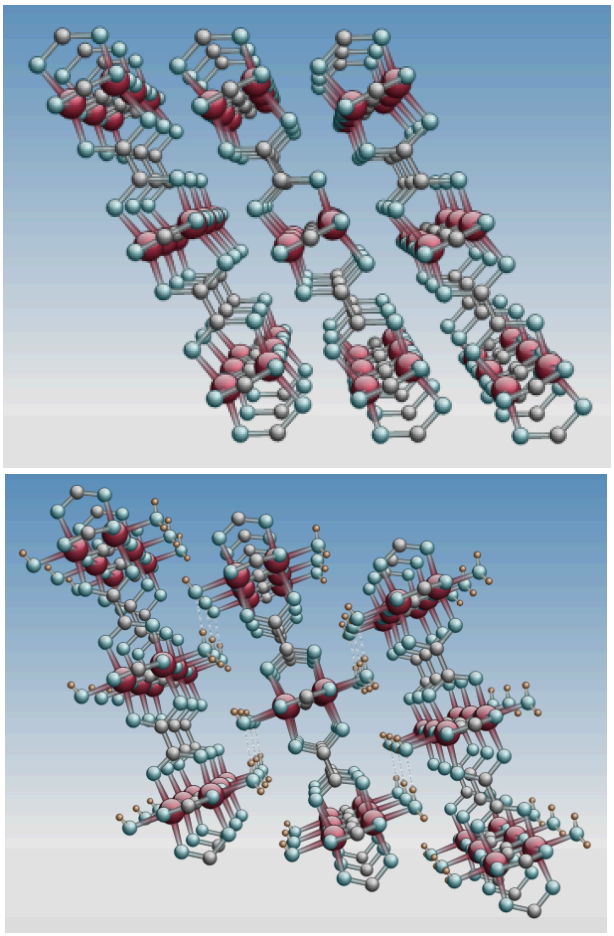

a.

b.

Figure 13. Ball and stick drawings representing 3x3x3 repeating unit cells looking along the c-axis for the proposed structures of **2,** in which (a) the oxalate oxygen atoms interact with the axial positions and (b) in which water molecules in the axial positions form a network of hydrogen bonding interactions (dashed lines) that knit the paddle-wheel layers together.

We have compared the simulated pXRDs (see supplementary materials) for both the MoC_2O_4 and $MoC_2O_4{\cdot}H_2O$ structures and note that both patterns are very similar, and dominated by the family of peaks at 2θ values of approximately 14°, 26°, 41° and 55°. The main differences in the simulated patterns for the two structures results from the relative intensities of these peaks, with the hydrate better approximating the ratios observed experimentally.

BET Surface Area Measurements

We have carried out BET surface area measurements for **2** (Fig. 14) in which the sample was initially degassed using a dynamic vacuum at 30°C for 12 h. After collecting the nitrogen adsorption data, the sample was again degassed, but at 100°, which resulted in an approximate 10% weight loss, consistent with the removal of the water of hydration as seen in the TGA results. The adsorption/desorption isotherms for both **2** and the anhydrous material are consistent with BET type II materials.[40],[41] The BET surface areas for **2** and the anhydrous material were found to be very similar, 4.85 m^2/g and 3.80 m^2/g, respectively, which is several orders of magnitude lower than is typically observed for MOFs containing larger linkers, such as terephthalate.[42] Likewise, the absorption average pore diameters for the hydrate and anhydrous materials were similar, having been measured to be 5.94 Å and 6.91 Å, respectively. This data is consistent with our proposed structure for **2,** in which the waters are axially coordinated and not located in the cavities formed by the paddle-wheel scaffolding. If the waters of hydration were located in the cavities, we would have anticipated a significant increase in the surface area and pore diameters upon dehydration. Alternatively, with the waters in the axial positions, the cavities created by the paddle-wheel scaffolding would not significantly change upon dehydration.

Electrical Resistance Measurements

We have attempted to measure the electrical resistance of a pressed pellet of **2**. Preliminary results suggest that the bulk material has an extremely high resistance (>10,000 Ω).

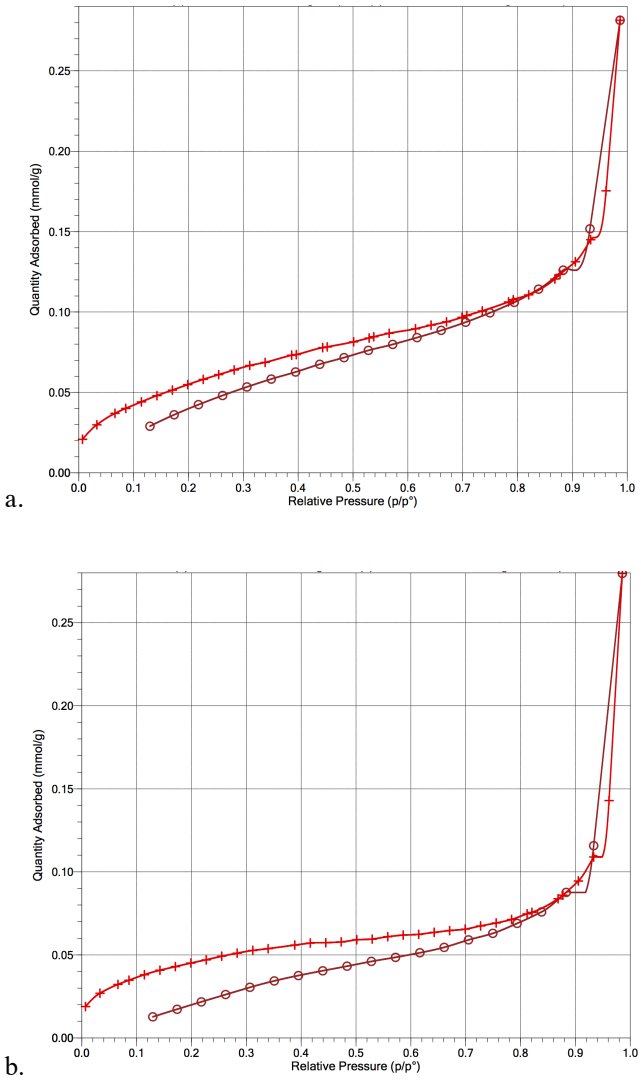

Figure 14. The linear nitrogen adsorption (+) and desorption (o) isotherms for **2** degassed *in vacuo* at (a) 30° and (b) 100°C.

We have not yet been able to investigate the effect of oxidation on the conductivity, which Bursten, Chisholm and D'Acchioli have suggested should result in an electronic band of appropriate width to produce metallic conductivity.[13] We are concerned that the near amorphous nature of our material may be a limiting factor that increases resistivity.[43]

Conclusions

We have been able to prepare a molybdenum(II) oxalate hydrate material by two different routes. Refluxing molybdenum(II) acetate with oxalic acid in aqueous solution for extended periods of time, followed by washing the resulting solid (**1**) with basic aqueous solution, produces **2**. Alternatively, **2** can be prepared directly from OCDM by

either refluxing potassium oxalate in aqueous solution for several hours, or by hydrothermal methods.

We have characterized **2** by a variety of physical methods and spectroscopic techniques to characterize the formulation and structure. This data suggests to us that the material consists of nearly amorphous or nanocrystalline particles of a relatively small oligomer in which there are connected layers of paddle-wheel like structures. It is not totally clear how the layers are connected, but we favor a structure in which axially coordinated water molecules form a hydrogen-bonding network. This is consistent with the IR, Raman, pXRD data and BET surface area measurements. Unfortunately, the EXAFS and pXRD results are somewhat ambiguous with respect to the location of the water molecules in the structure. Perhaps the most convincing evidence that argues against the conclusion that the waters of hydration are in the cavities, comes from the lack of a sharp non-hydrogen bonded O-H stretch in the IR spectrum of **2**, which is typically observed around 3600 cm^{-1} in other MOFs like MIL-53, when water is trapped in the pores.[44] Despite the absolute clarity concerning the waters of hydration, the totality of the results indicate that the Mo-Mo quadruple bond and paddle-wheel like structure comprises the dominant structural feature of these materials. Unfortunately, our data does not seem to be consistent with a highly extended electronic band structure which would facilitate delocalized communication between an extremely large number of Mo_2^{4+} units.

There are obvious limitations associated with these conclusions due to the nature of the particles that were produced. However, we are hopeful that we will be able to resolve some of these issues in the future and are actively pursuing alternative synthetic approaches that might produce larger, well defined crystals of other molybdenum(II) oxalate solvates. We are also interested in the potential for these materials to be electrochemically active,[45] since the precursor, molybdenum(II) acetate and Chisholm's oxalate dimer of dimers, have been shown to be oxidizable, forming interesting mixed valence complexes.[46] We anticipate that our molybdenum(II) oxalate materials will have analogous REDOX properties which would create holes in the highest occupied molecular orbital/band, which may induce the formation of a conducting material of some type. However, it is somewhat disturbing to note that Bursten, Chisholm and D'Acchioli had predicted that the Mo and W oxalate oligomeric system should be relatively easily oxidized,[13] based on electronic structure calculations. Unfortunately, this is not consistent with our observations concerning the relative air-stability of our molybdenum(II) oxalate hydrate, suggesting to us that the oxalate π-system mediated by the Mo-Mo δ-type orbitals are in fact not highly delocalized as we would have hoped. We suspect that this is due to rotation about the C-C bond of the oxalate, thus producing a disordered and nearly amorphous material. Further studies are in progress.

Experimental Section

General Methods

The preparation of the starting materials, molybdenum(II) acetate and potassium OCDM, have been described in detail elsewhere.[24,47] Combustion elemental analyses were performed by Atlantic Microlabs Inc., Norcross GA. Deionized water was prepared using an in-house ion-exchange system and degassed by bubbling UHP nitrogen into the liquid for one hour. All other chemicals and solvents were purchased from VWR and used without further purification.

IR samples were prepared by grinding a small amount of compound with dried spectral grade KBr using an agate mortar and pestle. The pellet was prepared using a screw bolt type pressed and produced nearly transparent pellets. The spectra were recorded using a Thermo Scientific Nicolet iS10 FT-IR spectrophotometer, in which air was recorded as a background and subtracted from the spectrum of the sample. Wavelengths were referenced to a thin film of polystyrene.

Samples for UV-Vis/NIR were prepared by diluting the pure powder of 2 to approximately 0.5%, 1% and 2% by weight in KBr, grinding using a mortar and pestle and pressing under 2 tons pressure to produce a 1 mm thick, 7 mm diameter pellet. Absorbance was computed by referencing the transmittance of a sample pellet to the

transmittance of a pure KBr pellet of the same thickness and diameter. The absorbance spectrum of **2** between 400 and 800 nm was recorded at 1 nm intervals using am Agilent Cary 300 UV-vis spectrophotometer. Diffuse transmission spectra were obtained between 800 and 2000 nm at 1 nm intervals using a Perkin-Elmer Lambda 950 (Perkin-Elmer, CT) UV/Vis/NIR spectrophotometer equipped with a LabSphere® 150 mm integrating sphere coated with spectralon. The sample was placed in front of the integrating sphere module and the diffuse spectra was acquired by the light being transmitted across the sphere.

SEM images and EDXS analysis were obtained using a powdered sample by sprinkling a small amount an aluminum SEM stub layered with double-sided carbon tape. The sample was coated with a 5.2 nm coating of iridium to help prevent charging. The sample was imaged and analyzed using a NanoSEM 630 FESEM (Thermo-Scientific, Hillsboro, OR). Images were taken at several different magnifications for comparison. EDXS analysis was performed using the X-Max detector (Oxford Instruments, Hillsboro, OR). EDXS analysis was collected using an accelerating voltage of 20 keV. The data collected is not quantitative. TEM was done using a Thermo Fisher Scientific Tecnai G2 LaB6 instrument. The TEM images and diffraction patterns were collected using 200 kV accelerating voltage. Beam exposure times were kept to a minimum in order to avoid potential beam damage.

Raman scattering was recorded using a Horiba LabRam HR Evolution with a 488 nm Ar^+ ion laser (Melles Griot) in back-scattered geometry. The incident power of the laser was kept below 500 uW and was focused on the sample using a 100x/NA 0.9 objective lens. The spectral resolution of the measurement was ~3 cm^{-1} using a 600 gr/mm grating and Synapse BIUVDD detector with 2048x512 pixel array.

TGA data was collected using a TA Instruments TGA-MS T5500 with a Discover mass spectrometer. Typically, an approximately 10 mg sample was loaded on the platinum pan in air and placed in the sample chamber, which was then purged with argon or nitrogen. The temperature range was from 20°C to 800°C, at a rate of 20°C/min.

Solid-state carbon-13 NMR spectra were recorded on a Bruker Avance-III-HD spectrometer using a double-resonance 4 mm HR-MAS probe, by collecting ~4k scans, at a spin rate of 13 kHz and a temperature of 298 K, with an inter-pulse delay of 15 s. The sample was ground to a fine powder using an agate mortar and pestle, packed into a rotor, fitted with a cap, and mounted in the MAS device.

XAFS samples were prepared by grinding the compound with sucrose as packing assist with a mortar and pestle, weighing out an amount calculated to give an absorption difference close to unity over the Mo K edge, and packing it into a slot in an aluminum holder, holding it in place and maintaining uniformity by a plastic tab press fit into the slot over it. The holder was attached to the base of a liquid N_2 cryostat so that the temperature is close to 80 K to reduce the Debye-Waller factors. Transmission spectra were measured on beamline 2-2 at the Stanford Synchrotron Radiation Lightsource in the continuous scanning mode. Spectra were calibrated internally by defining the first inflection point as 20007 eV, which is a good approximation for the energy of a lower valence Mo compound. Data were analyzed as described previously. Curve-fits were performed using amplitudes and phases calculated by the FEFF9 code.

PXRD data was collected on a Panalytical X'Pert Pro MPD system using Cu K-alpha radiation (1.54A) at 45 kV and 40 mA from 5-70 deg. 2-theta. Incident optics included a 1/4 deg. programmable divergence slit, 0.04 rad. Soller slit, 1/2 deg. anti-scatter slit and 10 mm beam mask. Diffracted optics include a 1/2 deg. programmable anti-scatter slit, a Ni filter and a PIXcel detector set to scanning line mode with an active length of 3.347 degrees. The programs CrystalMaker and CrystalDiffract were used to do initial simulations of the pXRD, which was then used in JADE to do the background correction and Rietveld refinement and PLATON was used to look for higher symmetry space groups.[48]

Synthesis of 1

Compound **1** can be prepared by refluxing molybdenum(II) acetate, which was ground to a fine powder in a mortar and pestle, with greater than two equivalents of oxalic acid dihydrate in degassed and deionized water for several days. If yellow needles of the molybdenum(II) acetate are used, the surface of the crystals will turn red, but the reaction will not go to completion. A typical reaction involves combining 0.500 g (1.17 mmol) of the yellow powdered $Mo_2(O_2CCH_3)$ with 0.980 g (7.77 mmol) $H_2C_2O_4{\cdot}2H_2O$ in a 100 mL round bottom flask, which was fitted with a reflux condenser and a nitrogen adaptor. The air was removed and replaced by UHP nitrogen using a dual manifold vacuum line. Approximately 50 mL of degassed and deionized water was added to the flask by transferring the liquid with positive pressure using a cannula. The mixture was refluxed for three days, producing a dark red powder. The mixture was vacuum filtered in air using a medium porosity sintered glass Buchner funnel and washed with deionized water, methanol and diethyl ether. The resulting solid was dried in a vacuum desiccator for 2 hours, producing 0.364 g, which was 77.1 % based on $Mo_2(O_2CCH_3)_4$ as the limiting reagent and an empirical formula of the product being $MoC_2O_4{\cdot}H_2O$.

Synthesis of 2

Preparation of **2** was most easily accomplished using a method similar to the preparation of **1**, by mixing 0.318 g (0.503 mmol) of red $K_4Mo_2Cl_8$, and 0.187 g (1.02 mmol) of $K_2C_2O_4.H_2O$ was place in a 50 mL round bottom flask that was fitted with a reflux condenser and a nitrogen adaptor. Using a dual manifold Schlenk type vacuum line, the flask was evacuated and filled with UHP nitrogen. Approximately 25 mL of degassed and distilled water was added to the round bottom flask using a cannula and the solution was heated to reflux for 24 hours. After heating, the mixture was vacuum filtered in air using a medium porosity sintered glass funnel. The dark maroon solid was washed with degassed and deionized water, until the filtrate was totally colorless. At that point the solid was washed with methanol and diethyl ether and dried in a vacuum desiccator, producing 0.183 g yield, which is 90.1% based on the potassium OCDM as the limiting reagent and the empirical formula for 2 being $MoC_2O_4{\cdot}H_2O$. It is also possible to prepare **2** by heating the mixture to 150 °C for 24 hours using a hydrothermal approach, using a Teflon lined autoclave that was loaded in a nitrogen filled glove-bag.

Synthesis of $MoC_2O_4{\cdot}$DMF

A typical preparation of $MoC_2O_4{\cdot}$DMF was accomplished using a hydrothermal method in which 0.250 g (0.396 mmol) of $K_4Mo_2Cl_8$ were combined with 0.149 g (0.810 mmol) of $K_2C_2O_4{\cdot}H_2O$ in the Teflon liner of an autoclave, using a glove bag that was filled with UHP nitrogen. The autoclave was sealed and place in an oven at 150 °C for 24 hours. After cooling to room temperature, the red solid was filtered in air, using a sintered glass frit and washed with water, methanol and diethyl ether. The solid was dried in vacuum for 2 hours providing 0.138 g, which is 86.3 % based on a formula of $MoC_2O_4{\cdot}$DMF. The FT-IR as a KBr pellet gives vibrations at 1654 (m), 1560 (s), 1410 (w), 1400 (mw), 1397 (w), 1302 (vs), 776 (m), and 587 (mw) cm^{-1}.

ASSOCIATED CONTENT

Supporting Information.

- TGA-MS analysis data
- XANES and EXAFS data simulation information
- pXRD and Crystallographic data (CIF)

AUTHOR INFORMATION

Corresponding Author

* E-mail: wgv102@psu.edu

Present Addresses

† Department of Chemistry and Environmental Science, Tiernan Hall - B006, New Jersey Institute of Technology, University Heights, Newark, New Jersey 07102, United States (C.N.P.)

Author Contributions

The manuscript was written through contributions of all authors.

Funding Sources

No competing financial interests have been declared. The Pennsylvania State University, Altoona, Office of Research and Sponsored Programs provided support through Undergraduate Research and Development grants. The PSU Materials Research Institute provided support through their Commonwealth Campuses Research Collaboration Development Program.

ACKNOWLEDGMENTS

This paper is dedicated to the memory of Malcolm H. Chisholm, may he rest in peace. We would also like to thank Dr. Richard Bell (PSU Altoona) and Dr. Alfred P. Satteleberger (ANL emeritus) for helpful discussions. Use of the Stanford Synchrotron Radiation Lightsource, SLAC National Accelerator Laboratory, is supported by the U.S. Department of Energy, Office of Science, Office of Basic Energy Sciences under Contract No. DE-AC01-76SF00515.

ABBREVIATIONS

MOF metal organic framework, COM calcium oxalate monohydrate, IR infrared, TGA thermogravimetric analysis, MS mass spectroscopy, SEM scanning electron micrograph, TEM transmission electron microscopy, DXS energy dispersive X-ray spectroscopy, DMF dimethylformamide, DFT Density Functional Theory, HOMO highest occupied molecular orbital, MAS magic angle spinning, pXRD powder X-ray diffraction, XANES X-ray absorption near edge structure, EXAFS extended x-ray absorption fine structure and BET Brunauer Emmett Teller theory.

For Table of Contents Only

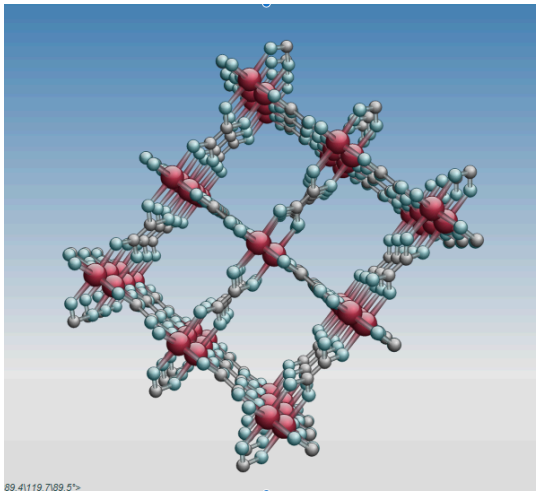

REFERENCES

[1] Köberl, M.; Cokoja, M.; Herrmann, W. A.; Kühn, F. E. From molecules to materials: molecular paddle-wheel synthons of macromolecules, cage compounds and metal-organic frameworks. *Dalton Trans.* **2011**, *40*, 6834 and reference therein.

[2] Cotton, F. A.; Norman, J. G.; Stults, B. R.; Webb, T. R. The Preparation and Crystal Structure of Dimolybdenum Tetraformate; Photoelectron Spectra of this and Several Other Dimolybdenum Tetracarboxylates. *J. Coord. Chem.* **1976**, *5*, 217.

[3] Robbins, G. A.; Martin, D. S. Crystal Structures of Tetrakis(μ-formato)dimolybdenum(II)-Potassium Chloride and Two New Polymorphs of Tetrakis(μ-formato)dimolybdenum(II). Single-Crystal Optical Absorption Spectra for Systems with the Molybdenum(II) Formate Dimers. *Inorg. Chem.* **1984**, *23*, 2086.

[4] Chisholm, M. H. Metal to metal multiple bonds in ordered assemblies *PNAS*, **2007**, *104*, 8, 2563.

[5] Mori, W.; Takamizawa, S. Microporous Materials of Metal Carboxylates. J. Solid State Chem. 2000, 152, 120.

[6] (a) Takamizawa, S.; Mori, W.; Furihata, M.; Takeda, S.; Yamaguchi, K. Synthesis and gas-occulsion properties of dinuclear molybdenum(II) dicarboxylates (furmarate, terephthalate, trans-trans-muconate, pyridine-2,5-dicarboxylate, and trans-1,4-cyclohexanedicarboxylate) *Inorg. Chim. Acta*, **1998**, *283*, 268; (b) Takamaizawa, S.; Furihata, M.; Takeda, S.; Yamaguchi, K.; Mori, W. Synthesis and Characterization of Novel Inclusion Complexes between Microporous Molybdenum(II) Dicarboxylates and Organic Polymers *Macromol.* **2000**, *33*, 6222

[7] Bell, D. S. The Promise of Metal-Organic Frameworks for use in Liquid Chromotography *LCGC North America*, **2018**, *36*, 6, 352.

[8] Pascanu, V.; Miera, G. G.; Inge, K.; Martin-Matute, B. M. Metal-Organic Frameworks as Catalysts for Organic Synthesis: A Critical Perspective J. Am. Chem. Soc., 2019, 141, 18, 7223.

[9] (a) Dolgopolova, E. A.; Brandt, A. J.; Ejegbavwo, O. A.; Duke, A. S.; Maddumapatabandi, T. D.; Galhenage, R. P.; Larson, B. W.; Reid, O. G.; Ammal, S. C.; Heyden, A.; Chandrashekhar, Mvs; Stavila, V.; Chem, D. A.; Shustova, N. B. Electronic Properties of Bimetallic Metal-Organic Frameworks (MOFs): Tailoring the Density of Electronic States through MOF Modularity. *J. Am. Chem. Soc.* **2017**, *139*, 14, 5201. (b) Stavila, V.; Talin, A. A.; Allendorf, M. D. MOF-based electronic and opto-electronic devices. *Chem. Soc. Rev.* **2014**, *43*, 5994. (c) Bhardwaj, S. K.; Bhardwaj, N.; Kaur, R.; Mehta, J.; Sharma, A. L.; Kim, K-H; Deep, A. An Overview of different strategies to introduce conductivity in metal-organic frameworks and miscellaneous applications thereof J. Mater. Chem. A, 2018, 6, 14992. (d) Aguilera-Sigalat, J.; Bradshaw, D. Synthesis and applications of metal-organic framework-quantum dot (QD@MOF) composites *Coord. Chem. Rev.* **2016**, *308*, 2, 267.

[10] (a) Cotton, F. A.; Murillo, C. A.; Young, M. D.; Yu, R.; Zhao, Q. Very large difference in electronic communication of dimetal species with heterobiphenylene and hetroanthracene. Inorg. Chem. 2008, 47, 219. (b) Cayton, R. H.; Chisholm, M. H. Electronic Coupling between Covalently Linked Metal-Metal Quadruple Bonds of Molybdenum and Tungsten. J. Am. Chem. Soc. 1989, 111, 8921. (c) Chisholm, M. H.; Patmore, N. Studies of Electronic Coupling and Mixed Valency in Metal-Metal Quadruply Bonded Complexes Linked by Dicarboxylate and Closely Related Ligands *Acc. Chem. Res.* **2007**, *40*, 1, 19.

[11] Cotton, F. A.; Murillo, C.; Walton, R. Multiple Bonds Between Metal Atoms, 3rd ed.; Springer Science and Business Media, 2005.

[12] Bursten, B. E.; Chisholm, M. H.; Hadad, C. M.; Li, J.; Wilson, P. J. M_2 δ-to-oxalate π*conjugation in oxalate-bridged complexes containing M-M quadruple bonds. *Chem. Comm.*, **2001**, 2382.

[13] (a) Bursten, B. E.; Chisholm, M. H.; D'Acchioli, J. S. Oxalate-Bridged Dinuclear M_2 Units: Dimers of Dimers, Cyclotetramers, and Extended Sheets (M = Mo, W, Tc, Ru, and Rh). Inorg. Chem., 2005, 44, 16, 5571. (b) Bursten, B. E.; Chisholm, M. H.; Hadad, C. M.; Li, J.; Wilson, P. J. Electronic Coupling Between Molybdenum and Tungsten Quadruple Bonds in Molecular Squares and extended Chains linked by Oxalate, Acetylenedicarboxylate and Perfluoroterephthalate Bridges *Irsl. J. Chem.*, **2001**, *41*, 187.

[14] Castro Neto, A. H.; Guinea, F.; Peres, N. M. R.; Novoselov, K. S.; Geim, A. K. The electronic properties of graphene *Rev. Mod. Phy.* **2009**, *81*, 109.

[15] Cotton, F. A.; Extine, M.; Rice, G. W. Sensitivity of the chromium-chromium quadruple bond in dichromium tetracarboxylate to axial coordination and changes in inductive effects. Inorg. Chem., 1978, 17, 1, 176.

[16] Lear, B. J.; Chisholm, M. H. Oxalate Bridged MM (MM = Mo_2, MoW, and W_2) Quadruply Bonded Complexes As Test Beds for Current Mixed Valence Theory: Looking beyond the Intervalence Charge Transfer Transition *Inorg. Chem.* **2009**, *48*, 23, 10954.

[17] (a) Mureinik, R. J. Synthesis and Characterization of Bis(Dicarboxylato)dimolybdnum(II) Compounds *J. Inorg. Nuc. Chem*, **1976**, *38*, 1275.

[18] The NIST data base reports the infrared spectrum of what is claimed to be molybdenum(II) oxalate monohydrate, whose empirical formula is $C_2H_2MoO_5$, but no further references are provided, NIST Chemistry WebBook, SRD69.

[19] Barber, G. D.; George, C.; Hogg, K.; Johnstone, S. T.; Pacheo, C. N.; Yennawar, H. P.; Van Der Sluys, W. G. Hydrothermal Synthesis and Structure of a Dinuclear Molybdenum(III) Squarate with a Mo-Mo Bond *ACS Omega*, **2020**, *5*, 4668.

[20] NIST Chemistry WebBook, 2018, https://webbook.nist.gov/cgi/cbook.cgi?ID=B6000058&Units=SI&Mask=80

[21] We note that when the MOF MIL-53(Al) is synthesized by hydrothermal methods, it initially incorporates benzene dicarboxylic acid into the pore structure. Loiseau, T.; Serre, C.; Huguenard, C.; Fink, G.; Taulelle, F.; Henry, M.; Bataille, T.; Ferey, G. A Rationale for the Large Breathing of the Porous Aluminum Terephthalate (MIL-53) Upon Hydration. Euro. J. Chem., 2004, 10, 6, 1373.

[22] Ogren, P. J. Using the Asymmetric Stretch Band of Atmospheric CO_2 to Obtain the C=O Bond Length *J. Chem. Ed.* **2002**, *79*, 1, 117.

[23] Finholt, J. E.; Leupin, P.; Sykes, A. G. Kinetics and Mechanism of Substitution of the Quadruply Bonded Molybdenum(II) Aquo Dimer with Thiocyanate and Oxalate Inorg. Chem. 1983, 22, 3315.

[24] Brencic, J. V.; Cotton, F. A. Preparation of some compounds containing multiple molybdenum-molybdenum bonds *Inorg. Chem.*, **1970**, *9*, 351.

[25] Cotton, F. A.; BertrM, A.; Pedersen, E.; Webb, T. R. Magnetic and Electrochemical properties of transition metal complexes with multiple meal-tometal bonds. III. Characterization of tetrapotassium and tripotassium tetrasulfatodimolybdates *Inorg. Chem.* **1975**, *14*, 391.

[26] Brencic, J. V.; Cotton, F. A. The Octachlorodimolybdate(II) Ion. A New Species with a Quadruple Metal-Metal Bond, *Inorg. Chem.*, **1969**, *8*, 1, 7.

[27] Dizayee, W.; Ying, M.; Griffin, J.; Alqahtani, M. S.; Buckley, A.; Fox, A. M.; Gehring, G. A.; Investigation of the distribution of localised and extended states in amorphous MoO_x *AIP Adv.* **2018**, *8,* 055118-1.

[28] Lawson-Wood, K.; Roberstson, I Study of the Decomposition of Calcium Oxalate Monohydrate using a Hyphenated Thermogravimetric Analyser-FT-IR System (TG-IR) **2016**, Perkin Elmer Inc., Application note.

[29] Dollimore, D. The Thermal Decomposition of Oxalates. A Review *Thermochimica Acta*, **1987**, *117*, 331.

[30] Bursten, B. E.; Clayton, T. W. A Simplified View of δ→ δ * Transition Energies in Compounds with multiple metal-metal bonds: The isolated δ - δ * manifold model J. Clus. Sci., 1994, 5, 157.

[31] Bursten, B. E.; Chisholm, M. H.; Clark, R. J. H.; Firth, S.; Hadad, C. M.; MacIntosh, A. M.; Wilson, P. J.; Woodward, P. M.; Zaleski, J. M. Oxalate-Bridged Complexes of Dimolybdenum and Ditungsten Supported by Pivalate Ligands: $(^tBuCO_2)_3M_2(\mu$-$O_2CCO_2)M_2(O_2C^tBu)_3$. Correlation of the Solid-State, Molecular, and Electronic Structures with Raman, Resonance Raman, and Electronic Spectral Data *J. Am. Chem. Soc.*, **2002**, *124*, 12, 3050.

[32] Spilker, T. F. Ph.D. dissertation, Chap. 3, Oxalate Bridged Quadruply Bonded Oligomers: Consideration of Electronic Structure and Synthetic Strategies, The Ohio State University 2014.

[33] See the discussion in chapter 16 and data in Table 16.11 of ref. 11. One should be cautious when interpreting the data for the molybdenum(II) formate hydrate. In chapter 4 the authors note that "The $Mo_2(O_2CH)_4$ molecule is also present in the monohydrate $Mo_2(O_2CH)_4{\cdot}H_2O$, which actually contains $Mo_2(O_2CH)_4$ and $Mo_2(O_2CH)_4{\cdot}(H_2O)_2$, units with Mo-Mo distances of 2.091(1) Å and 2.100(1) Å, respectively. In a subsequent study of the Raman and infrared spectra of $Mo_2(O_2CH)_4$ and $Mo_2(O_2CH)_4{\cdot}H_2O$, the investigators neglected to treat the hydrate as a mixture of the anhydrous and dihydrate forms." See Akhmedov, E. L.; Kotel'nikova, A. S.; Evstal'eva, O. N.; Kharitonov, Y. Y.; Smimov, A. N.; Tsivadze, A. Y.; Babievskaya, I. Z.; Abbasov, A, M. *Sov. J. Coord. Chem.* **1987**, *13*, 273.

[34] Cramer, S. P.; Eldem, P. K.; Paffett, M. T.; Winkler, J. R.; Dori, Z. Gray, H. B. X-ray Absorption Edge and EXAFS Spectroscopic Studies of Molybdenum Ions in Aqueous Solution *J. Am. Chem. Soc.* **1983**, *105*, 799.

[35] Fontaine, A. Trends of EXAFS and SEXAFS in Solid State Physics Ferreira, In J. G.; Ramos, M. T. (eds) X-ray Spectrscopy in Atomic and Solid State Physics. NATO ASI Series (Series B: Physics), 1988, vol 187, Springer, Boston MA.

ACS Paragon Plus Environment

[36] Conradson, S. D.; Schecker, J. XAFS A Technique to probe Local Structure Los Alamos Science, 26, 2000.

[37] F. A. Cotton and W. K. Bratton The molecular Structure of Molybdenum(II) Acetate *J. Am. Chem. Soc.* **1965**, *87*, 921.

[38] Cotton, F. A.; Mester, Z. C.; Webb, T. R. Acta Cryst., **1974**, B30, 2768.

[39] Holder, C. F., Schaak, R. E. Tutorial on Powder X-ray Diffraction for Characterizing Nanoscale Materials *ACS Nano*, **2019**, *13*, 7359.

[40] Brunauer, S.; Deming, L. S.; Deming, W. E.; Teller, E. On a Theory of the van der Waals Adsorption of Gases *J. Am. Chem. Soc*. **1940**, *62*, 1723.

[41] Bae, Y-S; Yazaydin, O.; Snurr, R. Q. Evaluation of the BET Method for Determining Surface Areas of MOFs and Zeolites that Contain Ultra-Micropores *Langmuir*, **2010**, *26*, 8, 5475.

[42] Walton, K. S.; Snurr, R. Q. Applicability of the BET Method for Determining Surface Areas of Microporous Metal-Organic Frameworks *J. Am. Chem. Soc*. **2007**, *129*, 8552.

[43] Day, R. W.; Bediako, D. K.; Rezaee, M.; Parent, L. R.; Skorupskii, G.; Arguilla, M. Q.; Hendron, C. H.; Stassen, I.; Gianneschi, N.; Kim, P.; Dinca, M. Single Crystals of Electrically Conductive Two-Dimensional Metal-Organic Frameworks: Structural and Electrical Transport Properties *ACS Cent. Sci*. 2019, 5, 12, 1959.

[44] Mounfield, W. P.; Walton, K. S. Synthesis of Large-Pore Stabilized MIL-53(Al) Compounds with Increased CO_2 Adsorption and Decreased Water Adsorption J. Mat. Chem., 2014, 00, 1.

[45] Morozan, A.; Jaouen, F. Metal organic frameworks for electrochemical applications *Energy & Envir. Sci*. ***2012**, 5, 9269*.

[46] Chisholm, M. H. Mixed valence complexes involving MM quadruple bonds (M = Mo or W) *Phil. Trans. R. Soc. A*, **2008**, *366*, 101.

[47] (a) Brignole, A.G.; Cotton, F.A., "Rhenium and Molybdenum compounds containing quadruple compounds" *Inorg. Synth*. **1972**, *13*, 81; (b) Pence, L. E.; Weisgerber, A. M.; Maounis, F.A.; "Synthesis of Molybdenum-Molybdenum Quadruple Bonds" *J. Chem. Educ*., **1999**, *76*, 404.

[48] Le Page, Y. Computer derivation of the symmetry elements implied in a structure description *J. App. Cyrst*. **1987**, *20*, 264.